A mutation in the ATP-binding site of the Kir6.2 subunit of the K_{ATP} channel alters coupling with the SUR2A subunit

Paolo Tammaro and Frances M. Ashcroft

Department of Physiology, Anatomy and Genetics, Oxford University, Oxford OX1 3PT, UK

Mutations in the pore-forming subunit of the ATP-sensitive K^+ (K_{ATP}) channel Kir6.2 cause neonatal diabetes. Understanding the molecular mechanism of action of these mutations has provided valuable insight into the relationship between the structure and function of the K_{ATP} channel. When Kir6.2 containing a mutation (F333I) in the putative ATP-binding site is coexpressed with the cardiac type of regulatory K_{ATP} channel subunit, SUR2A, the channel sensitivity to ATP inhibition is reduced and the intrinsic open probability (P_o) is increased. However, the extent of macroscopic current activation by MgADP was unaffected. Here we examine rundown and MgADP activation of wild-type and Kir6.2-F333I/SUR2A channels using single-channel recording, noise analysis and spectral analysis. We also compare the effect of mutating the adjacent residue, G334, on rundown and MgADP activation. All three approaches indicated that rundown of Kir6.2-F333I/SUR2A channels is due to a reduction in the number of active channels in the patch and that MgADP reactivation involves recruitment of inactive channels. In contrast, rundown and MgADP reactivation of wild-type and Kir6.2-G334D/SUR2A channels, and of Kir6.2-F333I/SUR1 channels, involve a gradual change in P_o. Our results suggest that F333 in Kir6.2 interacts functionally with SUR2A to modulate channel rundown and MgADP activation. This interaction is fairly specific as it is not disturbed when the adjacent residue (G334) is mutated. It is also not a consequence of the enhanced P_o of Kir6.2-F333I/SUR2A channels, as it is not found for other mutant channels with high P_o (Kir6.2-I296L/SUR2A).

(Resubmitted 15 August 2007; accepted after revision 6 September 2007; first published online 13 September 2007)
Corresponding author F. M. Ashcroft: Department of Physiology, Anatomy and Genetics, Parks Road, Oxford OX1 3PT, UK. Email: frances.ashcroft@physiol.ox.ac.uk

ATP-sensitive K^+ (K_{ATP}) channels couple cell metabolism to membrane electrical activity of the plasma membrane and thereby make an important contribution to many physiological processes (Ashcroft, 2005). Structurally, they are octameric complexes of two different proteins, SUR and Kir6.2 (Shyng & Nichols, 1997). Four inwardly rectifying K^+ channel subunits (usually Kir6.2) form a tetrameric pore (Inagaki *et al.* 1995; Sakura *et al.* 1995). Each Kir6.2 subunit is associated with a regulatory sulphonylurea receptor (SUR) subunit: SUR1 in pancreatic β-cells, SUR2A in cardiac and skeletal muscle and SUR2B in smooth muscle. Both subunits contribute to the metabolic regulation of K_{ATP} channel activity, which is mediated by changes in the intracellular concentrations of adenine nucleotides. Thus, binding of ATP or ADP (in both the presence or absence of Mg^{2+}) to Kir6.2 closes the channel (Tucker *et al.* 1997; Drain *et al.* 1998), whereas interaction of MgATP or MgADP with SUR (Nichols *et al.* 1996; Gribble *et al.* 1997; Shyng *et al.* 1997; Zingman *et al.* 2001) enhances channel opening.

Gain-of-function mutations in either Kir6.2 or SUR1 that impair channel inhibition by ATP give rise to neonatal diabetes (Ashcroft, 2005). One such mutation in Kir6.2 is F333I (Tammaro *et al.* 2005), which lies within the ATP-binding site in a homology model of Kir6.2 (Fig. 1). Interestingly, the functional effect of this mutation varied with the type of SUR subunit (Tammaro & Ashcroft, 2007). In particular, we found that the intrinsic open probability (P_o) of the channel (i.e. that in the absence of Mg^{2+}) was increased when Kir6.2-F333I was coexpressed with SUR2A but not with SUR1 (Tammaro & Ashcroft, 2007). Somewhat surprisingly however, given that Mg-nucleotides act by increasing P_o, the ability of MgADP and MgGDP to increase the macroscopic K_{ATP} current was similar for Kir6.2-F333I/SUR1 and Kir6.2-F333I/SUR2A (Tammaro & Ashcroft, 2007). Furthermore it was also similar for wild-type and mutant Kir6.2/SUR2A channels (Tammaro & Ashcroft, 2007).

This paper has online supplemental material.

 DOI: 10.1113/jphysiol.2007.143149

In this paper, we further explore the interaction of Mg-nucleotides with Kir6.2-F333I/SUR2A channels using single-channel recording and noise analysis. We also examine the functional effects of mutating the adjacent residue, Kir6.2-G334, on Kir6.2/SUR2A channels. A mutation at this position (G334D) is known to cause neonatal diabetes by dramatically reducing K_{ATP} channel ATP sensitivity (Masia *et al.* 2007).

We found that the F333I mutation influences MgADP activation of Kir6.2/SUR2A channels in a subtle way. Whereas MgADP reactivation of wild-type and G334D channels involves a change in P_o, MgADP activation of F333I channels is due to recruitment of channels from a gating conformation (or *mode*) in which P_o is very low to one in which P_o is high. Likewise, rundown of Kir6.2-F333I/SUR2A channels is associated with a sudden gating conformation switch in the opposite direction, from a high P_o to a P_o close to zero. These differences between F333I channels and both wild-type and G334D channels suggest that F333 may functionally interact with SUR2A to modulate rundown and MgADP activation. Furthermore, this interaction does not appear to involve the adjacent residue (G334).

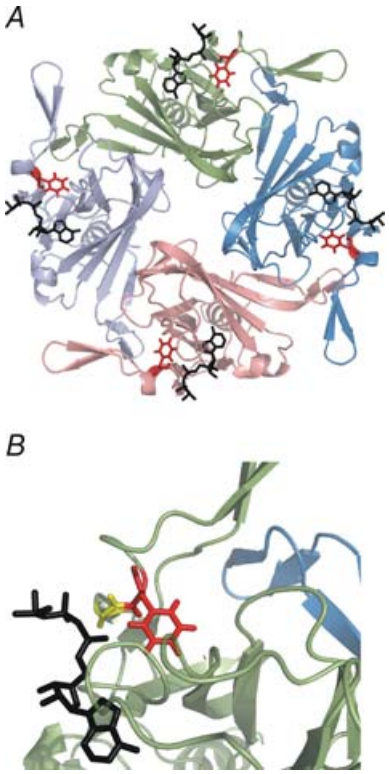

Figure 1. Homology model of the Kir6.2 tetramer
A, homology model of the Kir6.2 tetramer (Antcliff *et al.* 2005), viewed from below. For clarity, the transmembrane domains have been removed and each subunit is shown in a different colour. ATP (black, stick format) is shown docked into its four binding sites. F333 is shown in red. *B*, close up of the ATP-binding site showing F333 (red) and G334 (yellow).

Methods

Molecular biology

Human Kir6.2 (GenBank NM000525 with E23 and I377) and rat SUR2A (GenBank D83598) were used in this study. Site-directed mutagenesis of Kir6.2 and preparation of mRNA were performed as previously described (Tammaro & Ashcroft, 2007).

Oocyte preparation

Female *Xenopus laevis* were anaesthetized with MS222 (2 g l^{-1} added to the water). One ovary was removed via a mini-laparotomy, the incision sutured and the animal allowed to recover. Subsequently, animals were operated on for a second time, but under terminal anaesthesia. Immature stage V–VI oocytes were incubated for 60 min with 1 mg ml^{-1} collagenase (Sigma, type V) and manually defolliculated. All procedures were carried out in accordance with UK Home Office Legislations and the University of Oxford ethical guidelines. Oocytes were coinjected with ~0.8 ng wild-type or mutant Kir6.2 mRNA and ~4 ng of mRNA encoding SUR2A. The final injection volume was 50 nl per oocyte. Isolated oocytes were maintained in Barth's solution and studied 1–4 days after injection.

Electrophysiology

Currents were recorded from inside-out patches using an EPC10 amplifier (List Medical Electronics, Darmstadt, Germany) controlled with Pulse v8.74 software (Heka Electronik, Lambrecht, Germany). The pipette solution contained (mM): 140 KCl, 1.2 $MgCl_2$, 2.6 $CaCl_2$, 10 Hepes (pH 7.4 with KOH). The Mg-free internal (bath) solution contained (mM): 107 KCl, 1 K_2SO_4, 10 EGTA, 10 Hepes (pH 7.2 with KOH) and nucleotides as indicated. The Mg-containing internal solution was the same as the Mg-free solution but with the addition of 2 mM $MgCl_2$ and Mg-nucleotides (instead of K_2-nucleotides), as indicated. Experiments were conducted at 20–22°C. Solutions were changed using a local perfusion system consisting of tubes of ~200 μm diameter into which the tip of the patch pipette was inserted.

Single-channel analysis

Single-channel currents were recorded at −60 mV, filtered at 5 kHz and sampled at 20–50 kHz. Unitary amplitude and channel open probability (P_o) were measured from the Gaussian fits to all-points amplitude histograms. Traces were automatically idealized using a 50% threshold crossing method and open and closed dwell time distributions were fitted by a maximum likelihood criterion (Sigworth & Sine, 1987).

Stationary noise analysis and spectral analysis

Current traces of 200–800 ms duration were measured at −60 mV, low-pass filtered at 5 kHz using either an 8-pole Bessel filter (Frequency Devices Inc., MA, USA) or a 4-pole Butterworth filter, and digitized at 20 kHz. A bandwidth of 5 kHz was chosen to capture the fluctuations due to the briefest gating events (Conti, 1984; see online Supplementary material). Only patches exhibiting K_{ATP} current varying between ∼0.2 and ∼4 nA (immediately upon patch excision) were used for analysis. The baseline variance and the mean current obtained after complete block of the K_{ATP} current by 10 mM ATP (in the absence of Mg^{2+}) were subtracted from all data points. As Kir6.2-G334D channels are ATP insensitive (Li *et al.* 2000, 2005; Masia *et al.* 2007), baseline variance and the mean current were measured at 0 mV (the K^+ equilibrium potential).

For spectral analysis, 200 ms current recordings at −60 mV were filtered at 5 kHz and digitized at 20–50 kHz. For each power spectrum, a total of three to eight 200 ms-long traces were collected, Fourier transformed (using the fast Fourier transform algorithm with a window of 4096 or 8192 sample points), averaged and then log-binned with a bin-width of 0.02 before display. Spectra were fitted to the sum of two Lorentzian functions of the form:

$$S(f) = \frac{S_0}{1 + \frac{f^2}{f_c^2}}, \qquad (1)$$

where S_0 is a constant (the low frequency noise intercept), and f_c is the cut-off frequency.

Data analysis

Data were analysed with in-house routines developed in the IgorPro (Wavematrics, OR, USA) environment or using custom software (Dr M. Pusch, CNR, Italy). Data are given as mean ± S.E.M. Statistical significance was evaluated using Student's two-tailed t test and $P < 0.05$ taken to indicate a significant difference.

Results

Rundown and MgADP activation of wild-type and mutant channels

Immediately after establishing the inside-out patch configuration, the magnitude of the Kir6.2-F333I/SUR2A current increases sharply because the channel is no longer inhibited by intracellular ATP. Subsequently, the current declines with time (Fig. 2), a process known as rundown. However, rundown could be prevented by excising the patch into intracellular solution containing 100 μM MgADP (Fig. 2). One minute after excision, the current amplitude was reduced by 84 ± 3% ($n = 5$) in the absence and 25 ± 7% ($n = 5$) in the presence of MgADP, respectively.

A change in current magnitude could reflect a reduction in the channel open probability (P_o), in the single-channel current (i) or in the number of active channels in the patch (N). Single-channel recordings revealed that i does not change during rundown or MgADP reactivation: at −60 mV, the single-channel current was 4.1 ± 0.1 pA, 4.1 ± 0.1 pA and 4.0 ± 0.1 pA immediately upon patch excision, after rundown and in the presence of 100 μM MgADP, respectively ($n = 7$). We therefore explored if it is a change in P_o, in N, or in both, that underlies K_{ATP} channel rundown and MgADP activation.

We first recorded unitary currents from wild-type and mutant K_{ATP} channels. For simplicity, we refer to Kir6.2/SUR2A channels as wild-type, Kir6.2-G334D/SUR2A as G334D and Kir6.2-F333I/SUR2A as F333I channels. As Fig. 3 shows, rundown of wild-type and G334D channels manifests as a continuous reduction in P_o. In contrast, F333I channels show a very different behaviour (Figs 3 and 4). About 100 s after patch excision, first one channel and then another spontaneously closed, reducing the open probability abruptly to almost zero (Fig. 4). This represents the single-channel equivalent of the rundown seen for the macroscopic currents. Addition of MgADP caused the sudden activation of two channels to the full P_o (Fig. 4*A*).

If the channels gate independently, then the probability of seeing 1,2,3...N channels should follow the binomial theorem:

$$P(x) = \frac{N!}{x!(N-x)!} P_o^x (1 - P_o)^{(N-x)}, \qquad (2)$$

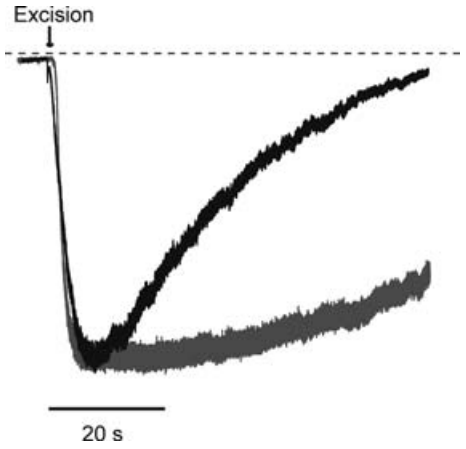

Figure 2. MgADP slows rundown
Macroscopic current recorded at −60 mV from a *Xenopus* oocyte coexpressing Kir6.2-F333I and SUR2A. The patch was excised at the time indicated by the arrow into intracellular solution with (grey) or without (black) MgADP (100 μM). Currents were obtained from separate patches on the same oocyte and have been normalized to allow visual comparison. The dashed line indicates the zero current level.

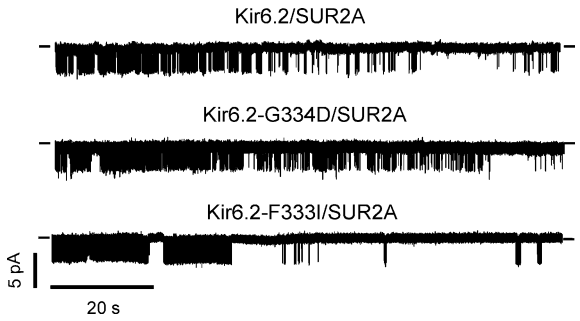

Figure 3. Effects of mutations on rundown of single-channel currents
Representative single-channel K_{ATP} currents recorded at −60 mV for inside-out patches from oocytes expressing SUR2A plus either wild-type or mutant Kir6.2, as indicated. Recordings started immediately upon patch excision.

where $P(x)$ is the probability that x channels are open out of a total of N. Figure 4*B* shows the best Gaussian fit to an all-points amplitude histogram of the single-channel current prior to rundown (left panel) and after addition of MgADP (right panel). Figure 4*C* shows the time spent at each current level (expressed as the area under each Gaussian peak) for the same tracts of current considered in Fig. 4*B*. The dots in Fig. 4*C* illustrate the fit of eqn (2) to the data using values of N and P_o of 2 and 0.76, and of 2 and 0.74, for currents recorded immediately after excision (indicated by *a* in Fig. 4*A*) and after activation by MgADP (*b* in Fig. 4*A*), respectively. In seven patches, mean values of P_o were 0.68 ± 0.04 immediately after excision and 0.70 ± 0.02 after MgADP activation, compared with almost zero (0.01 ± 0.01) after rundown. In two additional single-channel patches we did not observe a rapid switch of gating conformation during rundown.

To quantify the different modes of rundown of wild-type and mutant channels, we calculated the channel P_o in tracts of single-channel current of 30 s duration for 2 min following patch excision. Mean data are given in Fig. 5. It is evident that F333I channels undergo to an abrupt decrease in P_o during rundown in contrast to wild-type and G334D channels whose P_o declined progressively. When either Kir6.2-F333I or Kir6.2-G334D was coexpressed with SUR1, however, the P_o gradually decreased with time for both types of channel (Fig. 5). Thus the effect of the F333I mutation on rundown, like that on P_o, is specific for SUR2A.

These data provide direct evidence that changes in gating conformation occur during rundown and on MgADP activation of Kir6.2-F333I/SUR2A channels. However, they monitor the behaviour of only a few channels. We therefore next used noise analysis and spectral analysis to determine if the same phenomenon is true for the general channel population.

Noise analysis of rundown and MgADP activation

Stationary noise analysis (Neher & Stevens, 1977; DeFelice, 1981; Conti, 1984) assumes that there are N independent

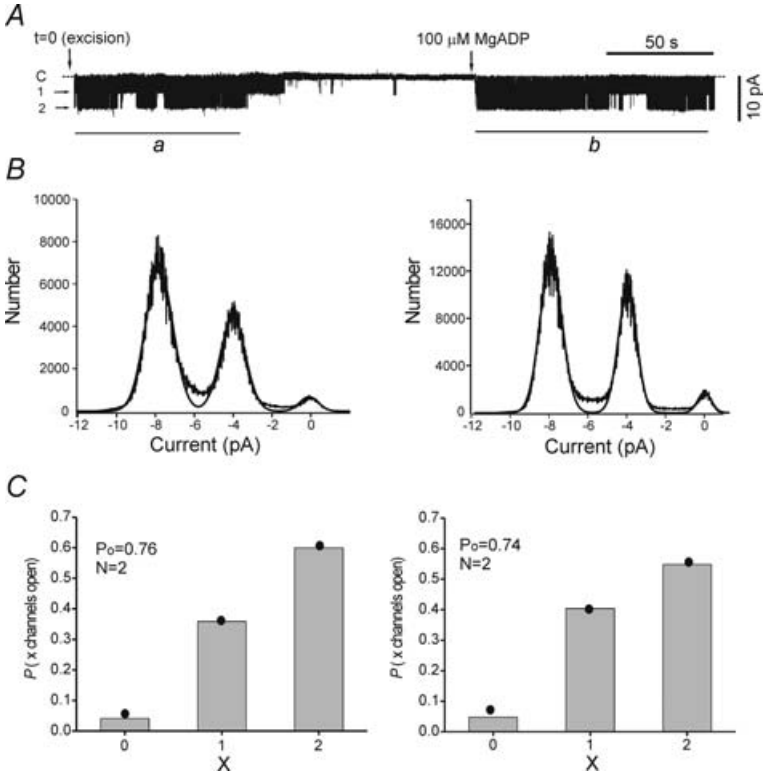

Figure 4. Unitary currents recorded from Kir6.2-F333I/SUR2A channels
A, single-channel Kir6.2-F333I/SUR2A currents recorded at −60 mV. The record started immediately after patch excision (arrowed). The maximum number of simultaneous openings seen in this patch was two; the arrows to the left of the current record indicate the number of channels open. The recording is representative of 7 separate experiments. *B*, all-points amplitude histograms from the same patch as in *A*: left panel, recorded after excision (indicated by *a* in *A*); right panel, in the presence of 100 μM MgADP (indicated by *b* in *A*). The continuous lines are the fit of the sum of 3 Gaussian functions. *C*, binomial analysis of the time spent at each open level for the tracts of current considered in *B* (*a* and *b* in *A*). Ordinate: probability that *x* channels are open. Abscissa: actual number of channels open (*x*). The histograms show the experimental probabilities calculated from the Gaussian fit to the amplitude histograms given in *B*. The filled dots show the probabilities obtained from the best fit of the data with eqn (2), with N and P_o equal to 2 and 0.76 (left panel) and 2 and 0.74 (right panel).

and identical channels with a single conducting level, *i*. The macroscopic current (I) is given by:

$$I = iNP_o. \quad (3)$$

From binomial theory, the variance, σ^2, is related to I by:

$$\sigma^2 = I(i - I/N) + \sigma_0^2 \quad (4)$$

where σ_0^2 is the variance at the zero current level (i.e. after block with 10 mM ATP).

Thus during graded changes in macroscopic current amplitude, such as those that occur during rundown or MgADP activation, a parabolic relationship between the current variance and the mean current is expected, provided that: (i) changes in macroscopic current amplitude are due to gradual changes in open probability; (ii) the single-channel current amplitude does not change; and (iii) the number of active channels in the patch membrane remains constant. As stated above, single-channel recordings revealed that i does not change during rundown or MgADP activation. Thus changes in I must be due to changes in P_o and/or N.

Figure 6 shows a typical noise analysis experiment on F333I channels. Following patch excision, the current progressively ran down, but it was restored by addition of 100 μM MgADP. This nucleotide concentration was chosen because it produces channel activation via SUR2A but no inhibition at the ATP-binding site on Kir6.2 (Tammaro & Ashcroft, 2007). Figure 6*B* illustrates a plot of the variance *versus* the mean current for 200 ms tracts of stationary current monitored during rundown: examples of these current tracts are shown in the right-hand panel of Fig. 6*A*. The parabolic curve (Fig. 6*B*) is an attempt to fit the data with eqn (4) by keeping i fixed at 4 pA (the measured value). It is clear that the data do not adequately fit. However, the data are well fitted by a straight line (Fig. 6*B*), as described by eqn (5) (see below). Figure 6*C* also demonstrates that data measured during MgADP-dependent activation lie on the same line as those for channel rundown, suggesting that similar mechanisms underlie both processes.

A linear relationship between the mean current and the variance is expected if the macroscopic current amplitude reflects changes in N rather then P_o. By combining eqns (3) and (4), we obtain (Jackson & Strange, 1995; Prakriya & Lewis, 2006):

$$\sigma^2 = Ni^2P_o(1 - P_o) + \sigma_0^2. \quad (5)$$

When P_o is constant this relationship is linear with a slope of $i(1 - P_o)$. The P_o calculated from a linear fit of the stationary noise analysis data was 0.76 ± 0.02 ($n = 7$), very close to the one we measured from single-channel recordings (0.68 ± 0.04, $n = 7$).

This analysis indicates that rundown and reactivation of F333I channels are caused by changes in N. In contrast, a graded change in P_o was found for wild-type channels using single-channel recording (see above) and has also been reported during rundown of native cardiac K_{ATP} channels (Alekseev *et al.* 1998). We therefore next performed noise analysis of wild-type channels during rundown (Fig. 7*A*). A plot of the variance *versus* the mean current, measured during rundown of the Kir6.2/SUR2A, revealed a *parabolic* trend. This suggests that rundown of recombinant wild-type channels is accompanied by a reduction in P_o as found in single-channel recordings (Alekseev *et al.* 1998).

The best fit of eqn (4) to the wild-type data gave an estimated value for i of 2.1 ± 0.2 pA ($n = 3$). This is an underestimate of the unitary amplitude measured from singe-channel recordings (4 pA, see above). Underestimation of the single-channel current might arise from excessive low-pass filtering: however, spectral analysis showed that the 5 kHz bandwidth used does not underestimate the variance (Supplemental Fig. 1). Another possible source of error could be if the tracts of stationary currents analysed were too short. To test if this was a problem, we fitted the current record with a polynomial function. For each current segment, we then took the mean of the polynomial and calculated the variance of the current around this mean (Silberberg & Magleby, 1993) (see Supplemental material). This correction slightly increased the estimated single-channel current (from 2.1 to 2.6 ± 0.2 pA, $n = 3$) but did not yield the value measured from the single-channel records.

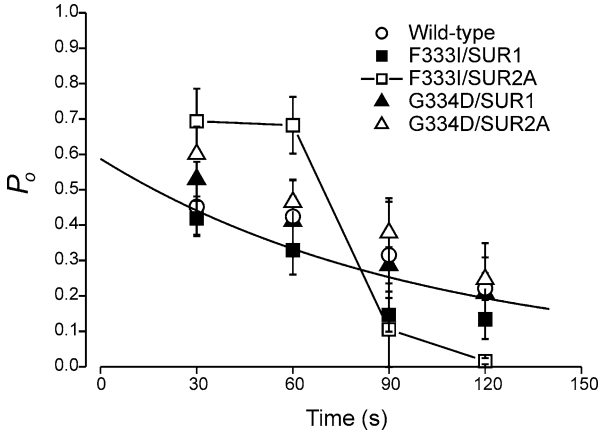

Figure 5. Channel open probability of wild-type and mutant channels during rundown
P_o was calculated for wild-type (Kir6.2/SUR2A) and mutant (as indicated) channels every 30 s following patch excision for a total of 2 min, and plotted *versus* time since excision. The number of experiments was 3–7 in each case. The continuous line is the best fit of the data with a single exponential function with a time constant of 100 s.

Thus for the wild-type channel the relationship between the variance and mean current follows a parabolic trend, but leads to an underestimation of the single-channel current amplitude. Our analysis suggests that this underestimate is not due to procedural errors, but most likely reflects the contribution of an additional process (other than a change in P_o) during rundown. The simplest explanation is that both P_o and N change during rundown of wild-type channels. In contrast, rundown of F333I channels is due only to a change in N.

We examined the relationship between current variance and mean current during rundown and reactivation of G334D channels. These channels were characterized by a substantial cell-attached current in macropatches, presumably due to the lower ATP sensitivity. After patch excision, G334D currents ran down (Fig. 7*B*) and were only partially restored by MgADP. Like wild-type channels, but in contrast to F333I channels, the relationship between current variance and mean current followed a parabolic trend ($i = 2.2 \pm 0.3$, $n = 4$). This implies P_o changes during rundown and reactivation of G334D channels, as it does in wild-type channels. Thus this gating conformation switch appears to be unique to F333I channels.

A possibility is that the peculiar conformation switching observed during rundown of F333I channels is related to the increased P_o (0.7) of the mutant channel. To test this, we used another Kir6.2 mutation that produces a very high P_o, both when expressed alone (0.7) or in combination with SUR (0.85; Proks *et al.* 2005). Figure 8 shows that Kir6.2-I296L/SUR2A currents ran down very little after patch excision ($< 4.4 \pm 2.5\%$, $n = 6$, in 1 min, compared with ~75% for F333I channels). Thus the change in gating mode of F333I channels during rundown is not simply a consequence of the enhanced P_o.

Effects of extracellular barium

If the linear relationship between the variance and the mean current found during rundown of F333I currents is due to a change in N at constant P_o, then a change in slope of this relationship is expected for a different value of

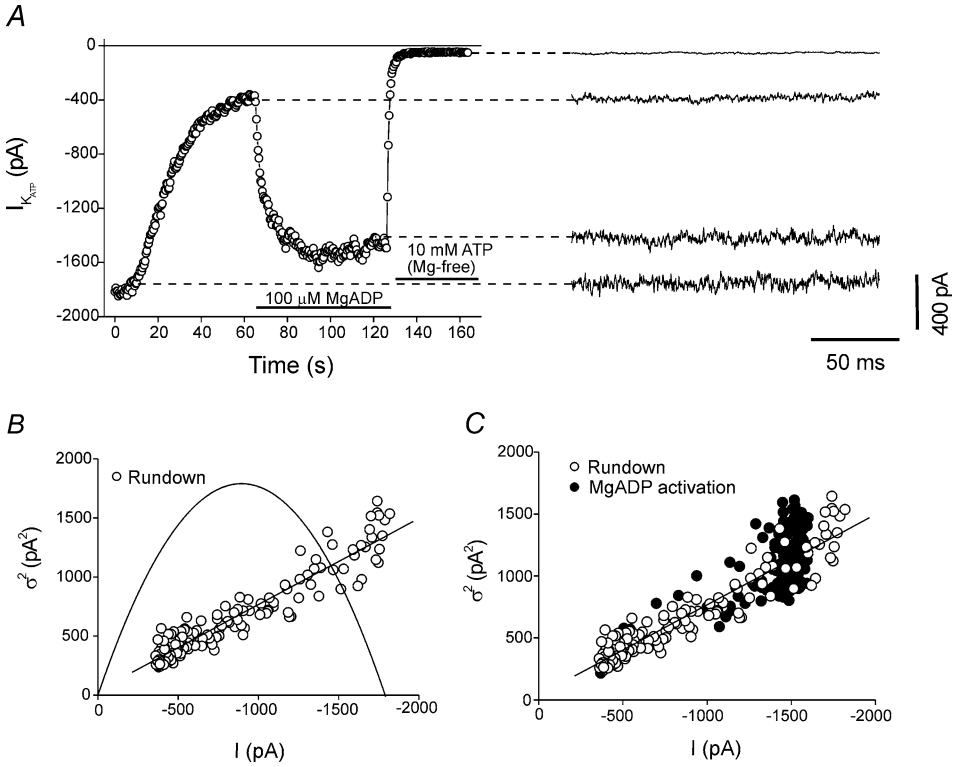

Figure 6. Stationary noise analysis of Kir6.2-F333I/SUR2A currents
A, mean current measured at −60 mV from 200 ms-long tracts of current plotted against the time since patch excision. Right panel shows examples of currents used for analysis. The dashed lines indicate the time at which each trace was recorded. *B*, current variance (σ^2) plotted against the mean current, measured during rundown. Same experiment as in *A*. The parabolic line is the best fit of eqn (4) to the data with i fixed at 4 pA. The straight line is the best fit of eqn (5) to the data, and gives a value for P_o of 0.80. *C*, current variance plotted against the mean current for the same patch as in *A*, measured during rundown (open circles) or MgADP activation (filled circles). The straight line is the same as in *B*.

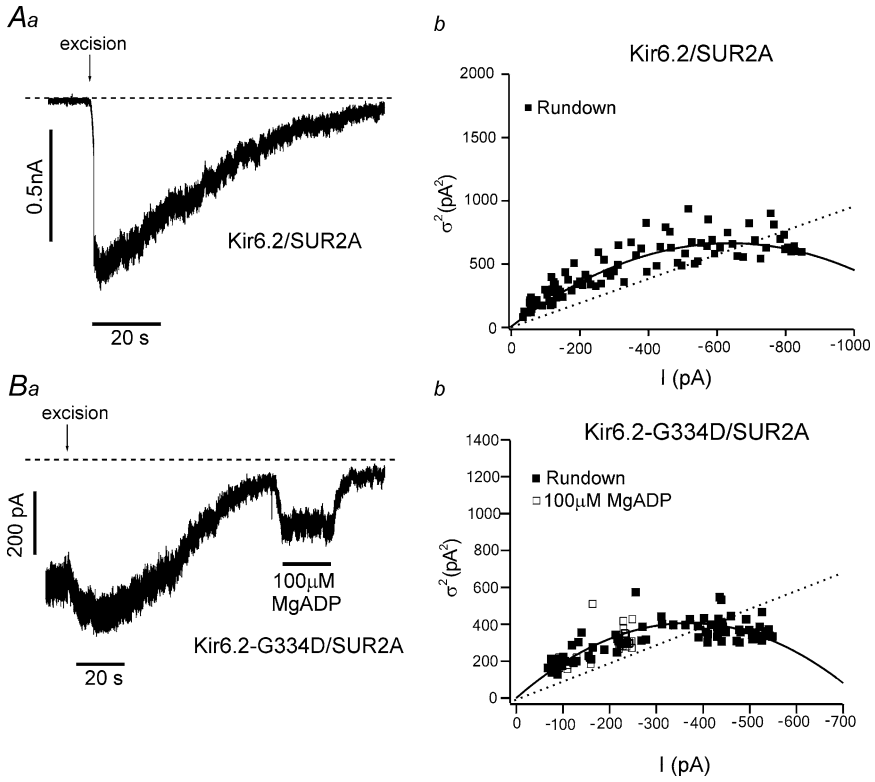

Figure 7. Rundown of Kir6.2/SUR2A and Kir6.2-G334D/SUR2A currents
Aa, macroscopic current recorded at −60 mV from a *Xenopus* oocyte coexpressing Kir6.2 and SUR2A. The patch was excised at the arrow. The dashed line indicates the zero current level. *Ab*, current variance (σ^2) plotted against the mean current, measured during rundown. Same experiment as in *Aa*. The parabolic line is the best fit of eqn (4) to the data. *Ba*, macroscopic current recorded at −60 mV from a *Xenopus* oocyte coexpressing Kir6.2-G334D and SUR2A. MgADP (100 μM) was applied as indicated. *Bb*, current variance (σ^2) plotted against the mean current, measured during rundown (filled symbols) and MgADP activation (open symbols). Same experiment as in *Ba*. The parabolic line is the best fit of eqn (4) to the data. The dotted lines in *Ab* and *Bb* represent the relationship between current variance and mean current observed for Kir6.2-F333I/SUR2A channels.

P_o. To test this idea, we used extracellular Ba^{2+} to decrease the K_{ATP} channel open probability.

It has been shown previously that Ba^{2+} reduces the P_o of native K_{ATP} channels in skeletal muscle without altering the single-channel current amplitude (Quayle *et al.* 1988). Figure 9*A* shows that K_{ATP} currents elicited by stepping the membrane from 0 mV to −60 mV are rapidly blocked in the presence of 300 μM external $BaCl_2$. The time constant of block was 7.6 ± 1.1 ms ($n = 4$), similar to that previously reported (Takano & Ashcroft, 1996). The steady-state current was characterized by a larger noise than that seen for currents of similar amplitude recorded in the absence of Ba^{2+} (compare Fig. 9*A*, upper and lower panels). Figure 9*B* illustrates two representative noise analysis experiments performed during current rundown in the presence and absence of Ba^{2+}. As predicted, the relationship between the variance and the mean current remains linear, but the slope is increased. The P_o derived from the linear fit of the noise data in the presence of Ba^{2+} was 0.33 ± 0.05 ($n = 4$), which is 43% of that measured in the absence of Ba^{2+}. This is in good agreement with the fact that the macroscopic F333I current in the presence of 300 μM Ba^{2+} is blocked by 46 ± 1% ($n = 4$).

Spectral analysis of rundown and MgADP activation

If changes in F333I current amplitude during rundown (or MgADP activation) are solely due to a reduction (or recruitment) of functional channels, then the power spectra must have the same frequency characteristics, whereas a change in P_o would alter the frequency components (Conti, 1984). Figure 9*C* illustrates spectra obtained before (open circles) and after (filled circles) current rundown. The spectra were well fitted with the sum of two Lorentzian functions with cut-off frequencies (f_c) of 11 and 490 Hz, and of 15 and 500 Hz, respectively. Similar f_c were seen after MgADP activation (Table 1).

In addition to supporting the idea that rundown and MgADP reactivation of Kir6.2-F333I/SUR2A are not associated with a marked change in channel gating,

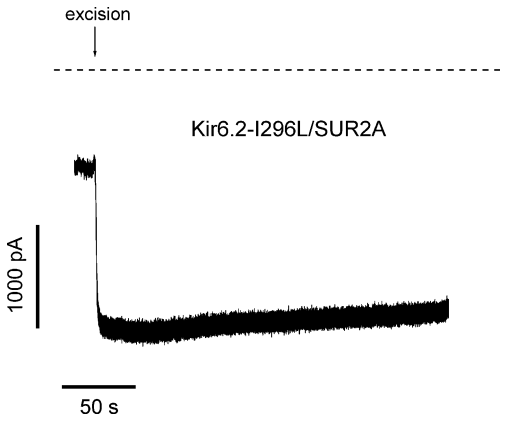

Figure 8. Rundown of Kir6.2-I296L/SUR2A currents
Macroscopic current recorded at −60 mV from a *Xenopus* oocyte coexpressing Kir6.2-I296L and SUR2A. The patch was excised at the arrow. The dashed line indicates the zero current level.

Table 1. Frequency characteristics of Kir6.2-F333I/SUR2A stationary current

	Before rundown		After rundown		100 μM MgADP	
$BaCl_2$ (μM)	Fast f_c (Hz)	Slow f_c (Hz)	Fast f_c (Hz)	Slow f_c (Hz)	Fast f_c (Hz)	Slow f_c (Hz)
0	514 ± 23 (7)	10.7 ± 1.3 (7)	551 ± 19 (7)	13.5 ± 2.8 (7)	517 ± 22 (7)	8.8 ± 1.3 (7)
300	559 ± 47 (4)	34 ± 2.3 (4)*	564 ± 34 (4)	31 ± 4.0 (4)*	531 ± 34 (4)	26 ± 2.4 (4)

Mean values of the cut-off frequencies (f_c) of the power spectra measured from 200 ms of stationary Kir6.2-F333I/SUR2A current recorded immediately upon patch excision ('before rundown'), after rundown, or in the presence of 100 μM MgADP, in both the absence or presence of 300 μM extracellular $BaCl_2$. *Statistical significance ($P < 0.01$) compared with the 0 mM $BaCl_2$ condition. The number of patches is indicated in parentheses.

spectral analysis provides information on the channel kinetics. Spectra recorded in the absence of Ba^{2+} immediately upon patch excision were well fitted with the sum of two Lorentzian functions. The presence of two components is expected for a channel characterized by bursts of opening separated by long closed times, which can be described by a simple three-state kinetic model (Scheme I, Supplemental material). From the open and closed time distributions measured during single-channel recordings, we obtained $\tau_o = 2.7 \pm 0.2$ ms,

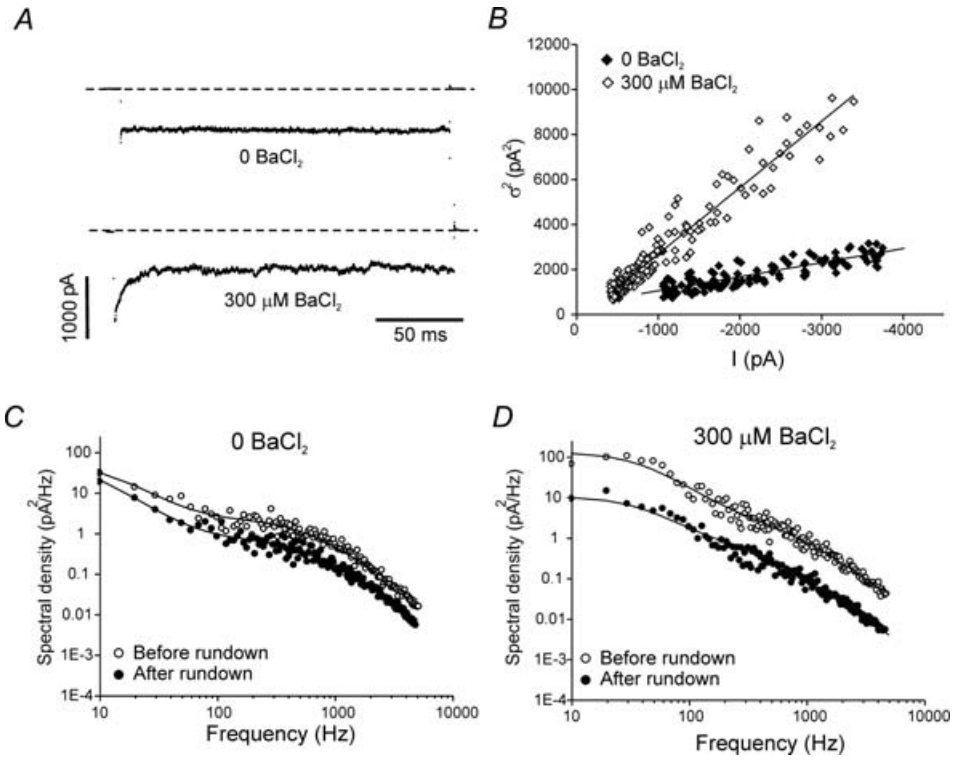

Figure 9. Stationary Kir6.2-F333I/SUR2A current noise analysis in the presence and absence of Ba^{2+}
A, representative current traces recorded in the absence (upper) or in the presence (lower) of extracellular Ba^{2+} (300 μM $BaCl_2$) in response to 200 ms pulses to −60 mV from a holding potential of 0 mV. The dashed line indicates the zero current level. *B*, stationary noise analysis, performed as indicated in the legend to Fig. 2, measured during rundown in the presence (open symbols) or absence (filled symbols) of Ba^{2+}. Data come from two different patches. The lines are the best fit of eqn (5) to the data with P_o equal to 0.32 (300 μM $BaCl_2$) and 0.70 (0 $BaCl_2$). *C*, power spectra measured from 200 ms tracts of stationary current recorded in the absence of $BaCl_2$ immediately upon patch excision (open circles) and after rundown (filled circles). Data are taken from the same patch as in *B* (filled diamonds). The continuous lines are the best fit of eqn (2) to the data, with f_c of 11 and 490 Hz and 15 and 500 Hz before and after rundown, respectively. *D*, power spectra measured from 200 ms tracts of stationary current recorded in the presence of 300 μM $BaCl_2$ before (open circles) or after (filled circles) rundown. Data are taken from the same patch as in *B* (open diamonds). The continuous lines are the best fit of eqn (2) to the data with f_c of 34 and 580 Hz and of 35 and 545 Hz before and after rundown, respectively.

$\tau_{C1} = 0.34 \pm 0.11$ ms, $\tau_{C2} = 15 \pm 8$ ms, $P_o = 0.7 \pm 0.2$ ($n = 5$). Rate constants calculated from these mean values (with Supplemental material eqns (1) to (4)) were: $k_1 = 344\ s^{-1}$, $k_{-1} = 2941\ s^{-1}$, $k_2 = 21\ s^{-1}$, $k_{-2} = 67\ s^{-1}$. We used these rate constants to calculate the predicted spectral cut-off frequencies (f_{cfast} and f_{cslow}) with Supplemental material eqns (5) and (6). The predicted values (14 and 523 Hz, respectively) were in good agreement with those (11 and 514 Hz, Table 1) measured from spectral analysis of the macroscopic currents.

In the presence of Ba^{2+}, spectra were also well fitted with the sum of two Lorentzian functions (Fig. 9*D*). The f_c were 34 and 580 Hz before, and 35 and 545 Hz after, current rundown (see Table 1 for mean data). The high frequency component was not significantly different in the presence and absence of Ba^{2+}, whereas the low frequency component was three times smaller in the absence of Ba^{2+} (Table 1). The low frequency component probably reflects interaction of Ba^{2+} with the open channel (Takano & Ashcroft, 1996). If Ba^{2+} acts as a channel blocker (Takano & Ashcroft, 1996) then the relaxation time constant τ_c is given by $1/(K_{off} + K_{on}[Ba^{2+}])$ and can be used to calculate f_c. The predicted corner frequency (~34 Hz) is in good agreement with that (~35 Hz) calculated using values for K_{on} (0.4 mM^{-1} ms^{-1}) and K_{off} (0.1 ms^{-1}) estimated from Takano & Ashcroft (1996).

Discussion

In this paper, we have investigated the biophysical basis of the rundown and MgADP activation of recombinant cardiac K_{ATP} channels containing the Kir6.2 mutation F333I. Single-channel recordings showed that *i* did not vary during either rundown or MgADP activation and three types of analysis – single-channel recording, noise analysis and spectral analysis – indicated that there was also no gradual change in P_o. Instead, both rundown and reactivation were associated with an abrupt switch in gating from a gating conformation with a high P_o to a gating conformation with a P_o close to zero and vice versa. In other words, the number (N) of functional Kir6.2-F333I/SUR2A channels was altered. Similar conversions between gating conformations have also been reported for other types of ion channels, such as CRAC channels (Prakriya & Lewis, 2006), volume-regulated Cl^- channels (Jackson & Strange, 1995) and voltage-gated sodium channels (e.g. Zhou *et al.* 1991; Keynes, 1994; Shcherbatko *et al.* 1999; Moran *et al.* 2003).

MgADP activation

Our data clearly show that MgADP produces a sudden change in the gating conformation of F333I channels which switch from a very low to a high P_o. However, this was not seen for either G334D channels or wild-type channels. The former finding suggests that the change in gating conformation is not related to the reduced inhibitory effect of ATP (and ADP) on F333I, as G334D channels are even less blocked by ATP/ADP. The fact the mutation of the adjacent residue (G334) does not cause a gating conformation switch also suggests that mutations in this region are unlikely to be associated with gross conformational changes. Rather the data support a specific interaction of F333I with SUR2A that modulates the channel gating conformation when the nucleotide-binding domains (NBDs) of SUR2 are occupied by MgADP.

Rundown

Rundown of wild-type and G334D channels involves a gradual change in P_o (and probably also in N), whereas rundown of F333I channels appears to be mediated almost entirely by an abrupt change in P_o. What might underlie this difference in rundown? We do not know the answer to this question. Indeed the molecular mechanism of rundown of wild-type channels remains unclear. A number of factors have been proposed to cause rundown of wild-type K_{ATP} channels, including hydrolysis of PIP_2 (Hilgemann & Ball, 1996), channel dephosphorylation (Ribalet *et al.* 2000), and protease activity. A role for these processes in the later phases of rundown cannot be excluded. However, the fact that MgADP is able to reactivate partially rundown currents and that rundown is slowed by MgADP suggest that MgADP may play a role: for example, by dissociating from the NBDs of SUR following patch excision.

We considered the possibility that the different pattern of rundown of F333I channels is a consequence of the higher intrinsic P_o. For example, if the affinity of F333I for PIP_2 were increased, this would both enhance P_o and, due to a reduced rate of PIP_2 dissociation on patch excision, lead to a much slower decline in P_o (or even no decline at all) (Li *et al.* 2000, 2005). This would be consistent with the fact that G334D channels have a normal P_o (Drain *et al.* 1998; Masia *et al.* 2007) and that the P_o of these channels declines during rundown as it does for wild-type channels. It would also be consistent with the fact that when coexpressed with SUR1, rundown of F333I channels resembles that of wild-type channels. However, this idea is untenable, because a similar gating switch was not observed for another mutant channel (Kir6.2-I296L/SUR2A) with an enhanced P_o.

Alternatively, the different properties of rundown found for F333I channels may reflect a difference in coupling of Kir6.2 to SUR2A. This is conceivable, given that in homology models of Kir6.2 (Antcliff *et al.* 2005; Li *et al.* 2005) residue F333 lies on the outer part of the Kir6.2 tetramer in a position in which it could interact with SUR

(Fig. 1). Further support for this idea comes from the fact that F333 sits very close to the N-terminus of the adjacent Kir6.2 subunit. The N-terminus appears to be involved in interactions between Kir6.2 and SUR as mutations and/or deletions in this region alter channel gating in the presence but not absence of SUR (Babenko *et al.* 1999; Reimann *et al.* 1999). This further suggests that F333 might lie close to SUR in the 3-dimensional structure of the octameric K_{ATP} channel complex, consistent with its predicted location on the outer surface of Kir6.2.

In conclusion, we have demonstrated that mutation of F333 in the putative ATP-binding site of Kir6.2 influences rundown and MgADP activation. This effect is fairly specific as it is not observed when the adjacent residue (G334) is mutated. Thus despite the fact that the F333I mutation does not influence the extent of Mg-nucleotide activation (Tammaro & Ashcroft, 2007), the underlying mechanism appears to differ for wild-type and mutant channels.

References

Alekseev AE, Brady PA & Terzic A (1998). Ligand-insensitive state of cardiac ATP-sensitive K^+ channels. Basis for channel opening. *J Gen Physiol* **111**, 381–394.

Antcliff JF, Haider S, Proks P, Sansom MS & Ashcroft FM (2005). Functional analysis of a structural model of the ATP-binding site of the K_{ATP} channel Kir6.2 subunit. *EMBO J* **24**, 229–239.

Ashcroft FM (2005). ATP-sensitive potassium channelopathies: focus on insulin secretion. *J Clin Invest* **115**, 2047–2058.

Babenko AP, Gonzalez G & Bryan J (1999). The N-terminus of KIR6.2 limits spontaneous bursting and modulates the ATP-inhibition of K_{ATP} channels. *Biochem Biophys Res Commun* **255**, 231–238.

Conti F (1984). Noise analysis and single-channel recordings. In *Current Topics in Membranes and Transport*, vol. 22, pp. 371–405. Academic Press, London.

DeFelice LJ (1981). *Introduction to Membrane Noise*. Plenum, New York.

Drain P, Li L & Wang J (1998). K_{ATP} channel inhibition by ATP requires distinct functional domains of the cytoplasmic C terminus of the pore-forming subunit. *Proc Natl Acad Sci U S A* **95**, 13953–13958.

Gribble FM, Tucker SJ & Ashcroft FM (1997). The essential role of the Walker A motifs of SUR1 in K_{ATP} channel activation by MgADP and diazoxide. *EMBO J* **16**, 1145–1152.

Hilgemann DW & Ball R (1996). Regulation of cardiac Na^+,Ca^{2+} exchange and K_{ATP} potassium channels by PIP_2. *Science* **273**, 956–959.

Inagaki N, Gonoi T, Clement JP 4th, Namba N, Inazawa J, Gonzalez G, Aguilar-Bryan L, Seino S & Bryan J (1995). Reconstitution of IK_{ATP}: an inward rectifier subunit plus the sulfonylurea receptor. *Science* **270**, 1166–1170.

Jackson PS & Strange K (1995). Single-channel properties of a volume-sensitive anion conductance. Current activation occurs by abrupt switching of closed channels to an open state. *J Gen Physiol* **105**, 643–660.

Keynes RD (1994). Bimodal gating of the Na^+ channel. *Trends Neurosci* **17**, 58–61.

Li L, Geng X, Yonkunas M, Su A, Densmore E, Tang P & Drain P (2005). Ligand-dependent linkage of the ATP site to inhibition gate closure in the K_{ATP} channel. *J Gen Physiol* **126**, 285–299.

Li L, Wang J & Drain P (2000). The I182 region of k(ir) 6.2 is closely associated with ligand binding in K_{ATP} channel inhibition by ATP. *Biophys J* **79**, 841–852.

Masia R, Koster JC, Tumini S, Chiarelli F, Colombo C, Nichols CG & Barbetti F (2007). An ATP-binding mutation (G334D) in KCNJ11 is associated with a sulfonylurea-insensitive form of developmental delay, epilepsy, and neonatal diabetes. *Diabetes* **56**, 328–336.

Moran O, Conti F & Tammaro P (2003). Sodium channel heterologous expression in mammalian cells and the role of the endogenous β1-subunits. *Neurosci Lett* **336**, 175–179.

Neher E & Stevens CF (1977). Conductance fluctuations and ionic pores in membranes. *Annu Rev Biophys Bioeng* **6**, 345–381.

Nichols CG, Shyng SL, Nestorowicz A, Glaser B, Clement JP 4th, Gonzalez G, Aguilar-Bryan L, Permutt MA & Bryan J (1996). Adenosine diphosphate as an intracellular regulator of insulin secretion. *Science* **272**, 1785–1787.

Prakriya M & Lewis RS (2006). Regulation of CRAC channel activity by recruitment of silent channels to a high open-probability gating mode. *J Gen Physiol* **128**, 373–386.

Proks P, Girard C, Haider S, Gloyn AL, Hattersley AT, Sansom MS & Ashcroft FM (2005). A gating mutation at the internal mouth of the Kir6.2 pore is associated with DEND syndrome. *EMBO Rep* **6**, 470–475.

Quayle JM, Standen NB & Stanfield PR (1988). The voltage-dependent block of ATP-sensitive potassium channels of frog skeletal muscle by caesium and barium ions. *J Physiol* **405**, 677–697.

Reimann F, Tucker SJ, Proks P & Ashcroft FM (1999). Involvement of the N-terminus of Kir6.2 in coupling to the sulphonylurea receptor. *J Physiol* **518**, 325–336.

Ribalet B, John SA & Weiss JN (2000). Regulation of cloned ATP-sensitive K channels by phosphorylation, MgADP, and phosphatidylinositol bisphosphate (PIP_2): a study of channel rundown and reactivation. *J Gen Physiol* **116**, 391–410.

Sakura H, Ammala C, Smith PA, Gribble FM & Ashcroft FM (1995). Cloning and functional expression of the cDNA encoding a novel ATP-sensitive potassium channel subunit expressed in pancreatic β-cells, brain, heart and skeletal muscle. *FEBS Lett* **377**, 338–344.

Shcherbatko A, Ono F, Mandel G & Brehm P (1999). Voltage-dependent sodium channel function is regulated through membrane mechanics. *Biophys J* **77**, 1945–1959.

Shyng S, Ferrigni T & Nichols CG (1997). Regulation of K_{ATP} channel activity by diazoxide and MgADP. Distinct functions of the two nucleotide binding folds of the sulfonylurea receptor. *J Gen Physiol* **110**, 643–654.

Shyng S & Nichols CG (1997). Octameric stoichiometry of the K_{ATP} channel complex. *J Gen Physiol* **110**, 655–664.

Sigworth FJ & Sine SM (1987). Data transformations for improved display and fitting of single-channel dwell time histograms. *Biophys J* **52**, 1047–1054.

Silberberg SD & Magleby KL (1993). Preventing errors when estimating single channel properties from the analysis of current fluctuations. *Biophys J* **65**, 1570–1584.

Takano M & Ashcroft FM (1996). The Ba^{2+} block of the ATP-sensitive K^+ current of mouse pancreatic β-cells. *Pflugers Arch* **431**, 625–631.

Tammaro P & Ashcroft F (2007). The Kir6.2-F333I mutation differentially modulates K_{ATP} channels composed of SUR1 or SUR2 subunits. *J Physiol* **581**, 1259–1269.

Tammaro P, Girard C, Molnes J, Njolstad PR & Ashcroft FM (2005). Kir6.2 mutations causing neonatal diabetes provide new insights into Kir6.2–SUR1 interactions. *EMBO J* **24**, 2318–2330.

Tucker SJ, Gribble FM, Zhao C, Trapp S & Ashcroft FM (1997). Truncation of Kir6.2 produces ATP-sensitive K^+ channels in the absence of the sulphonylurea receptor. *Nature* **387**, 179–183.

Zhou JY, Potts JF, Trimmer JS, Agnew WS & Sigworth FJ (1991). Multiple gating modes and the effect of modulating factors on the microI sodium channel. *Neuron* **7**, 775–785.

Zingman LV, Alekseev AE, Bienengraeber M, Hodgson D, Karger AB, Dzeja PP & Terzic A (2001). Signaling in channel/enzyme multimers: ATPase transitions in SUR module gate ATP-sensitive K^+ conductance. *Neuron* **31**, 233–245.

Acknowledgements

We thank Michael Pusch and Chris Miller for critical discussions. We thank the Wellcome Trust and the Royal Society for support. F.M.A. is a Royal Society Research Professor. P.T. holds a Junior Research Fellowship at Wolfson College.

Supplemental material

Online supplemental material for this paper can be accessed at:
http://jp.physoc.org/cgi/content/full/jphysiol.2007.143149/DC1
and
http://www.blackwell-synergy.com/doi/suppl/10.1113/jphysiol.2007.143149